Figure S1

A

Age group	Anterior	Posterior	Salivary
9-11gw	10x Anterior segments	12x Posterior segments	_____
12-13gw	66x Anterior tooth germs	51x Molar tooth germs	7x Submandibular SG
14-16gw	50x Anterior tooth germs 24x Molars tooth germs	_____	3x Submandibular SG
17-19gw	40x Anterior tooth germs	17x Molar tooth germs	4x Submandibular SG
20-22gw	45x Anterior tooth germs	19x Molar tooth germs	_____

B

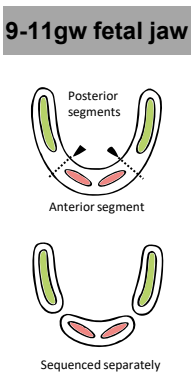

C

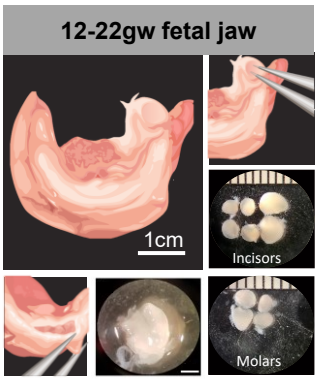

D

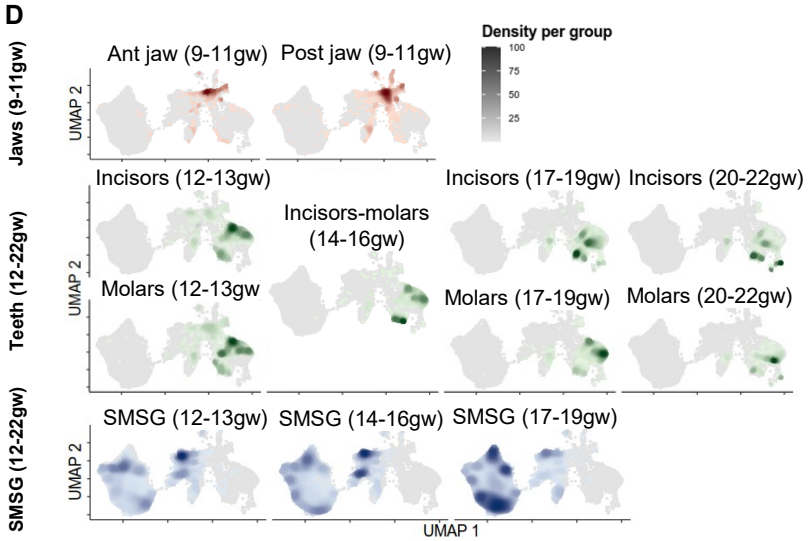

F

Sequencing Depth

	Overall QC
Total reads	274558788
Total UMIs	120304751
Duplication rate	56.17%
Cells with >100 UMIs	145258
Cells with >200 UMIs	96072
Mean UMIs per cell	455
Mean genes per cell	373
Percentage of mitochondrial UMIs per cell	1.38%

E

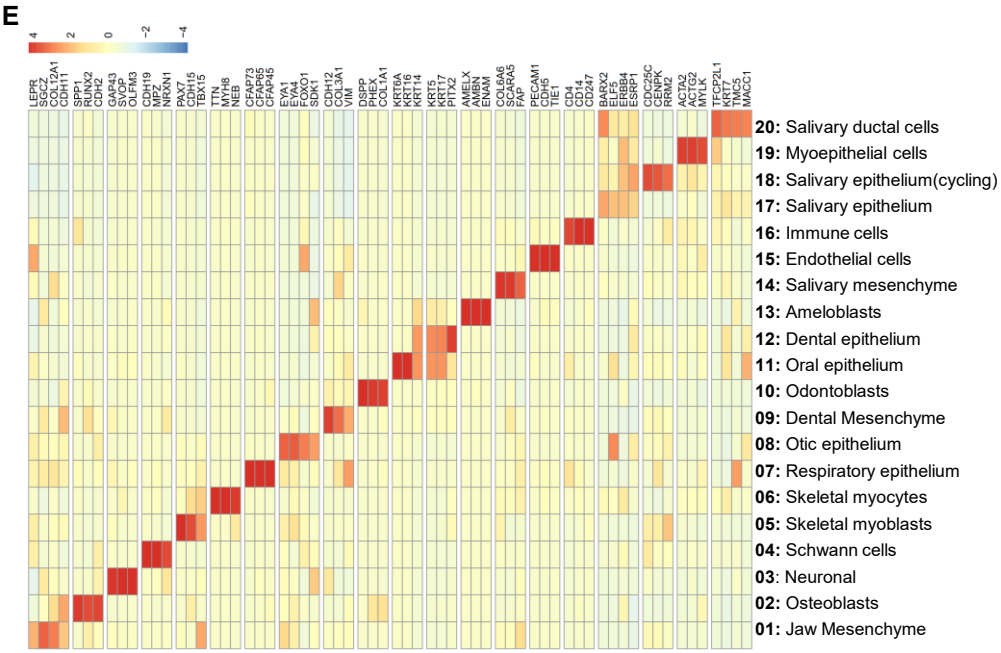

Figure S2

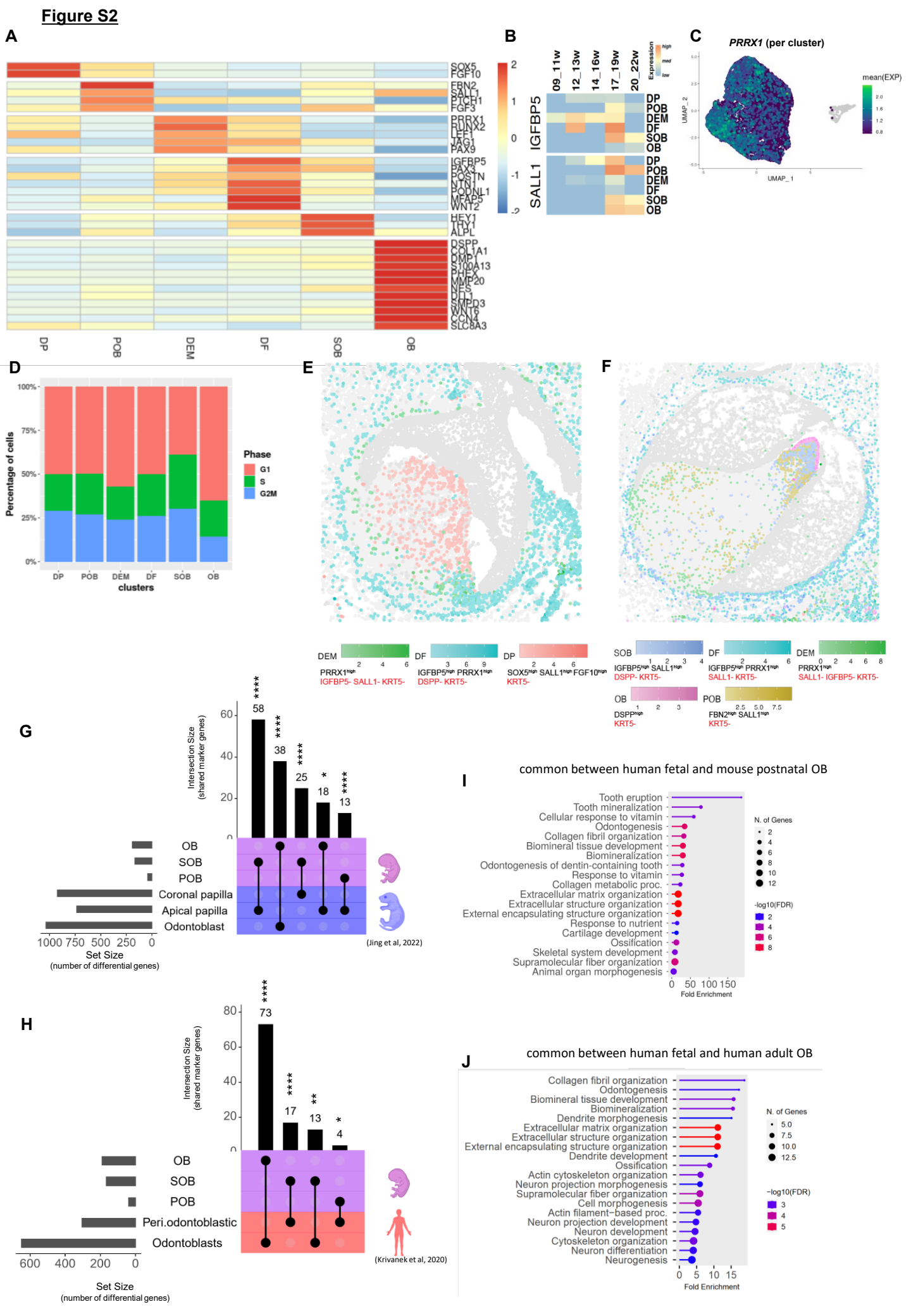
A
SOX5
FGF10
FBN2
SALL1
PTCH1
FGF3
PRRX1
RUNX2
LEF1
TAG1
PAX9
IGFBP5
PAX3
POSTN
NTN1
PODNL1
MFAP5
WNT2
HEY1
TRY1
ALPL
DSPP
COL1A1
DMP1
SYNDA13
PHEX
MMP20
NYES
DTN1
SMPD3
WNT6
CCN4
SLC8A3
DP
POB
DEM
DF
SOB
OB
B
09_11w
12_13w
14_16w
17_19w
20_22w
Expression
high
med
low
IGFBP5
SALL1
DP
POB
DEM
DF
SOB
OB
C
PRRX1 (per cluster)
mean(EXP)
UMAP_2
UMAP_1
D
Percentage of cells
100%
75%
50%
25%
0%
DP
POB
DEM
DF
SOB
OB
clusters
Phase
G1
S
G2M
E
DEM
PRRX1high
IGFBP5- SALL1- KRT5-
DF
IGFBP5high PRRX1high
DSPP- KRT5-
DP
SOX5high SALL1high FGF10high
KRT5-
F
SOB
IGFBP5high SALL1high
DSPP- KRT5-
DF
IGFBP5high PRRX1high
SALL1- KRT5-
DEM
PRRX1high
SALL1- IGFBP5- KRT5-
OB
DSPPhigh
KRT5-
POB
FBN2high SALL1high
KRT5-
G
Intersection Size
(shared marker genes)
58
38
25
18
13
****
****
****
*
****
OB
SOB
POB
Coronal papilla
Apical papilla
Odontoblast
Set Size
(number of differential genes)
(Jing et al, 2022)
H
Intersection Size
(shared marker genes)
73
17
13
4
****
****
**
*
OB
SOB
POB
Peri.odontoblastic
Odontoblasts
Set Size
(number of differential genes)
(Krivanek et al, 2020)
I
common between human fetal and mouse postnatal OB
Tooth eruption
Tooth mineralization
Cellular response to vitamin
Odontogenesis
Collagen fibril organization
Biomineral tissue development
Biomineralization
Odontogenesis of dentin-containing tooth
Response to vitamin
Collagen metabolic proc.
Extracellular matrix organization
Extracellular structure organization
External encapsulating structure organization
Response to nutrient
Cartilage development
Ossification
Skeletal system development
Supramolecular fiber organization
Animal organ morphogenesis
Fold Enrichment
N. of Genes
-log10(FDR)
J
common between human fetal and human adult OB
Collagen fibril organization
Odontogenesis
Biomineral tissue development
Biomineralization
Dendrite morphogenesis
Extracellular matrix organization
Extracellular structure organization
External encapsulating structure organization
Dendrite development
Ossification
Actin cytoskeleton organization
Neuron projection morphogenesis
Supramolecular fiber organization
Cell morphogenesis
Actin filament−based proc.
Neuron projection development
Neuron development
Cytoskeleton organization
Neuron differentiation
Neurogenesis
Fold Enrichment
N. of Genes
−log10(FDR)

Figure S3

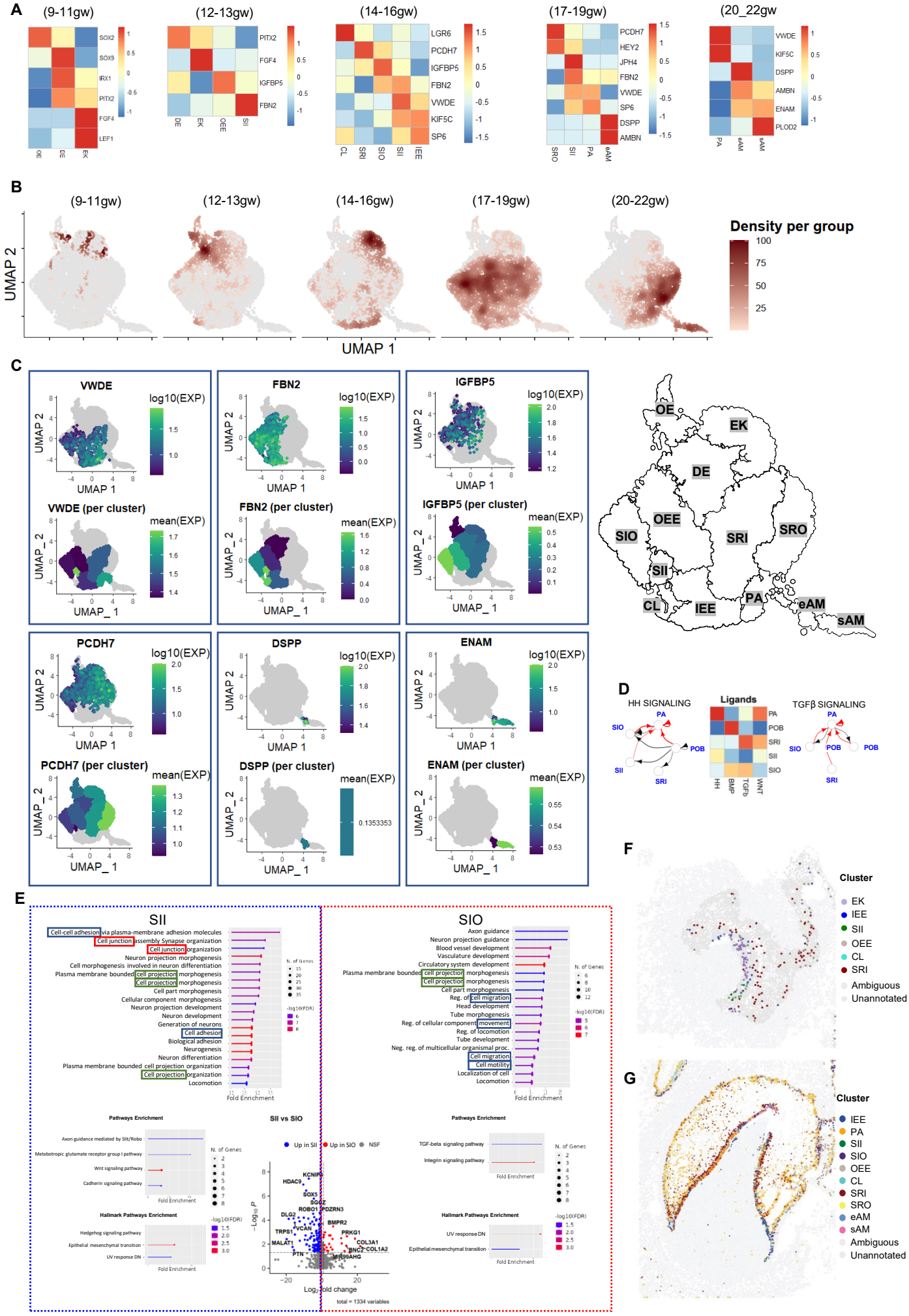
A
(9-11gw)
(12-13gw)
(14-16gw)
(17-19gw)
(20_22gw
SOX2
SOX9
IRX1
PITX2
FGF4
LEF1
OE
DE
EK
PITX2
FGF4
IGFBP5
FBN2
OE
DE
EK
OEE
SII
LGR6
PCDH7
IGFBP5
FBN2
VWDE
KIF5C
SP6
CL
SRI
SIO
SII
IEE
PCDH7
HEY2
JPH4
FBN2
VWDE
SP6
DSPP
AMBN
SRO
SII
PA
eAM
VWDE
KIF5C
DSPP
AMBN
ENAM
PLOD2
PA
eAM
sAM
B
(9-11gw)
(12-13gw)
(14-16gw)
(17-19gw)
(20-22gw)
UMAP 2
UMAP 1
Density per group
100
75
50
25
C
VWDE
log10(EXP)
VWDE (per cluster)
mean(EXP)
FBN2
log10(EXP)
FBN2 (per cluster)
mean(EXP)
IGFBP5
log10(EXP)
IGFBP5 (per cluster)
mean(EXP)
PCDH7
log10(EXP)
PCDH7 (per cluster)
mean(EXP)
DSPP
log10(EXP)
DSPP (per cluster)
mean(EXP)
0.1353353
ENAM
log10(EXP)
ENAM (per cluster)
mean(EXP)
UMAP 1
UMAP_1
UMAP 2
UMAP_2
OE
EK
DE
OEE
SIO
SRI
SRO
SII
CL
IEE
PA
eAM
sAM
D
HH SIGNALING
Ligands
TGFβ SIGNALING
PA
SIO
POB
SII
SRI
HH
BMP
TGFb
WNT
E
SII
Cell-cell adhesion via plasma-membrane adhesion molecules
Cell junction assembly Synapse organization
Cell junction organization
Neuron projection morphogenesis
Cell morphogenesis involved in neuron differentiation
Plasma membrane bounded cell projection morphogenesis
Cell projection morphogenesis
Cell part morphogenesis
Cellular component morphogenesis
Neuron projection development
Neuron development
Generation of neurons
Cell adhesion
Biological adhesion
Neurogenesis
Neuron differentiation
Plasma membrane bounded cell projection organization
Cell projection organization
Locomotion
N. of Genes
-log10(FDR)
Fold Enrichment
SIO
Axon guidance
Neuron projection guidance
Blood vessel development
Vasculature development
Circulatory system development
Plasma membrane bounded cell projection morphogenesis
Cell projection morphogenesis
Cell part morphogenesis
Reg. of Cell migration
Head development
Tube morphogenesis
Reg. of cellular component movement
Reg. of locomotion
Tube development
Neg. reg. of multicellular organismal proc.
Cell migration
Cell motility
Localization of cell
Locomotion
Pathways Enrichment
Axon guidance mediated by Slit/Robo
Metabotropic glutamate receptor group I pathway
Wnt signaling pathway
Cadherin signaling pathway
Hallmark Pathways Enrichment
Hedgehog signaling pathway
Epithelial mesenchymal transition
UV response DN
SII vs SIO
Up in SII
Up in SIO
NSF
KCNIP3
HDAC9
SOX5
SGCZ
ROBO1
PDZRN3
DLG2
VCAN
BMPR2
TRPS1
PRKG1
MALAT1
COL3A1
BNC2
COL1A2
PTN
MIR99AHG
−Log10 P
Log2 fold change
total = 1334 variables
TGF-beta signaling pathway
Integrin signaling pathway
F
Cluster
EK
IEE
SII
OEE
CL
SRI
Ambiguous
Unannotated
G
Cluster
IEE
PA
SII
SIO
OEE
CL
SRI
SRO
eAM
sAM
Ambiguous
Unannotated

Figure S4

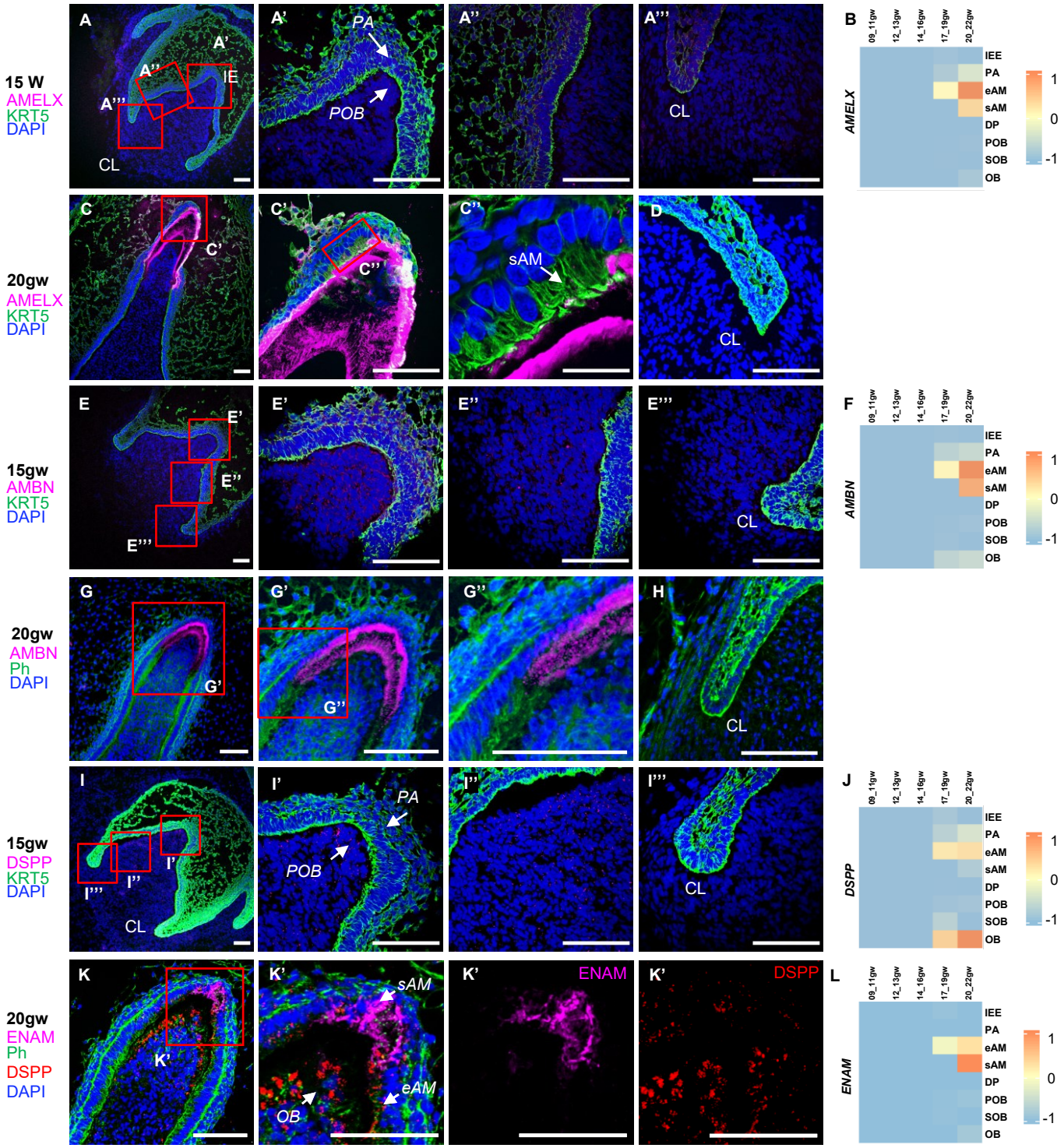

M

Protein level	eAM	sAM	OB
DSPP	+	-	+++
AMBN	+	+	-
AMELX	+	+	-
ENAM	-	+	-

A

Figure S5

Step 1: Selecting all support cells present at the same timepoint as progenitor cells

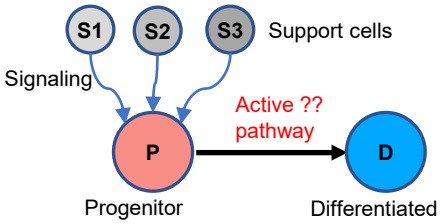

Step 2: Analyze ligand:recptor interactions using *talklr*

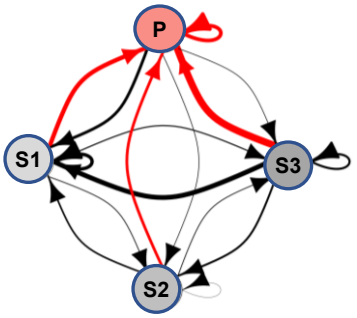

- Only signals received by progenitor cells are considered. (red lines)

- Only literature supported interactions of major pathways are considered

Step 3: Differentially expressed genes (DEGs) between progenitor and differentiated cells

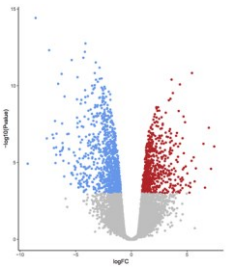

- By DEsingle package

- DEGs are used as downstream targets to infer pathway activity.

Step 4: Model the downstream network by *scMLnet*

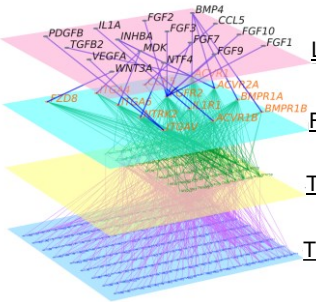

Ligands: expressed in support cells

Receptors: expressed in progenitor

TFs: expressed in progenitor

Target genes: DEGs

Step 5: Assign fold-change values to target genes and aggregate scores from bottom to top

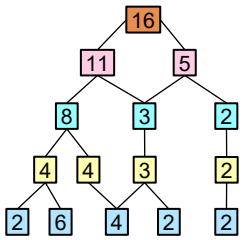

Pathway: sums of Lig

Lig: sums of Rec

Rec: sums of TFs

TF: means of targets

Target: fold change

*scores are normalized to interaction library depth

Step 6: Rank pathways based on overall activity score

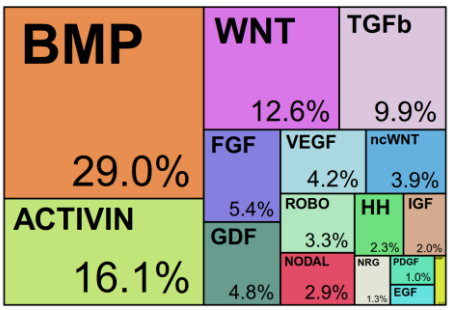

B

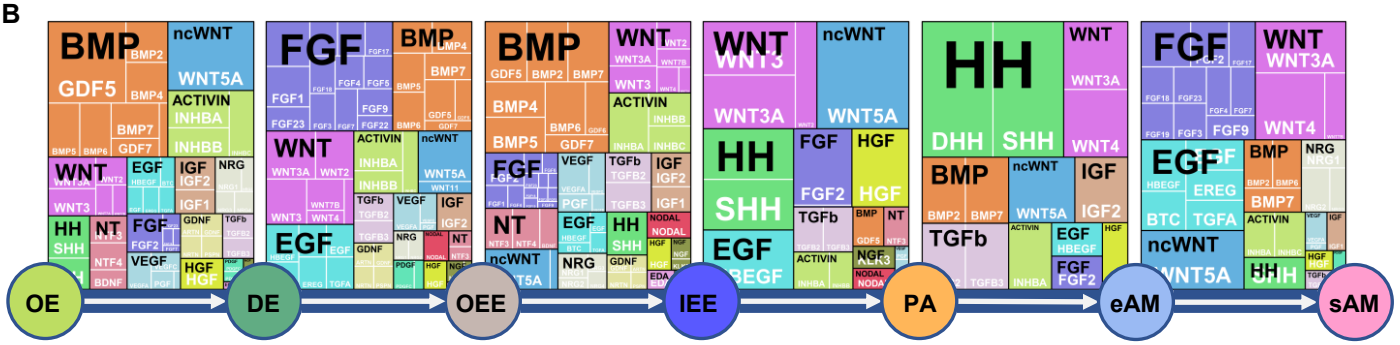

C

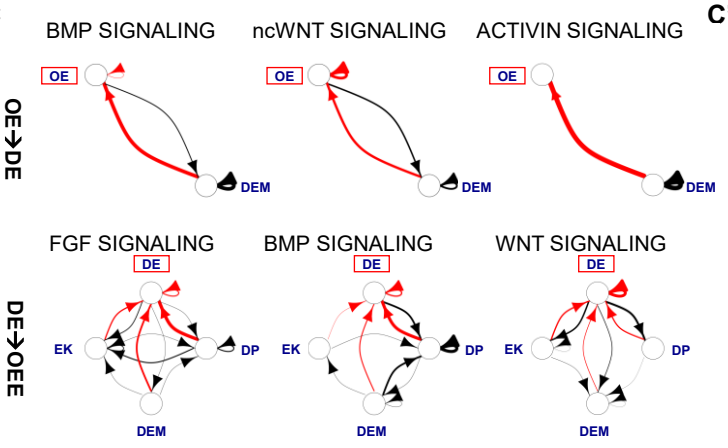

C''

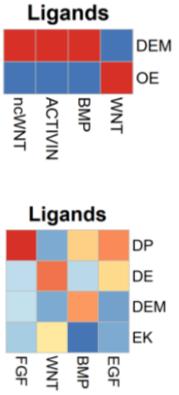

C'''

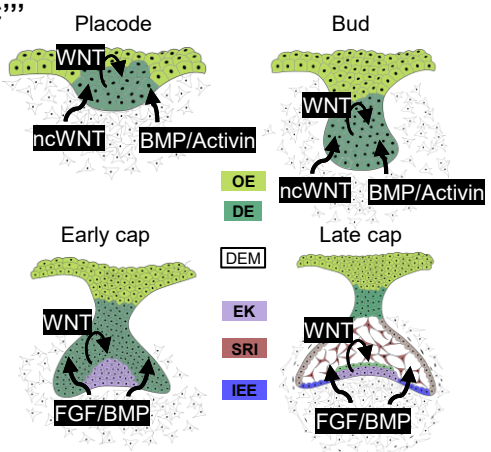

Figure S6

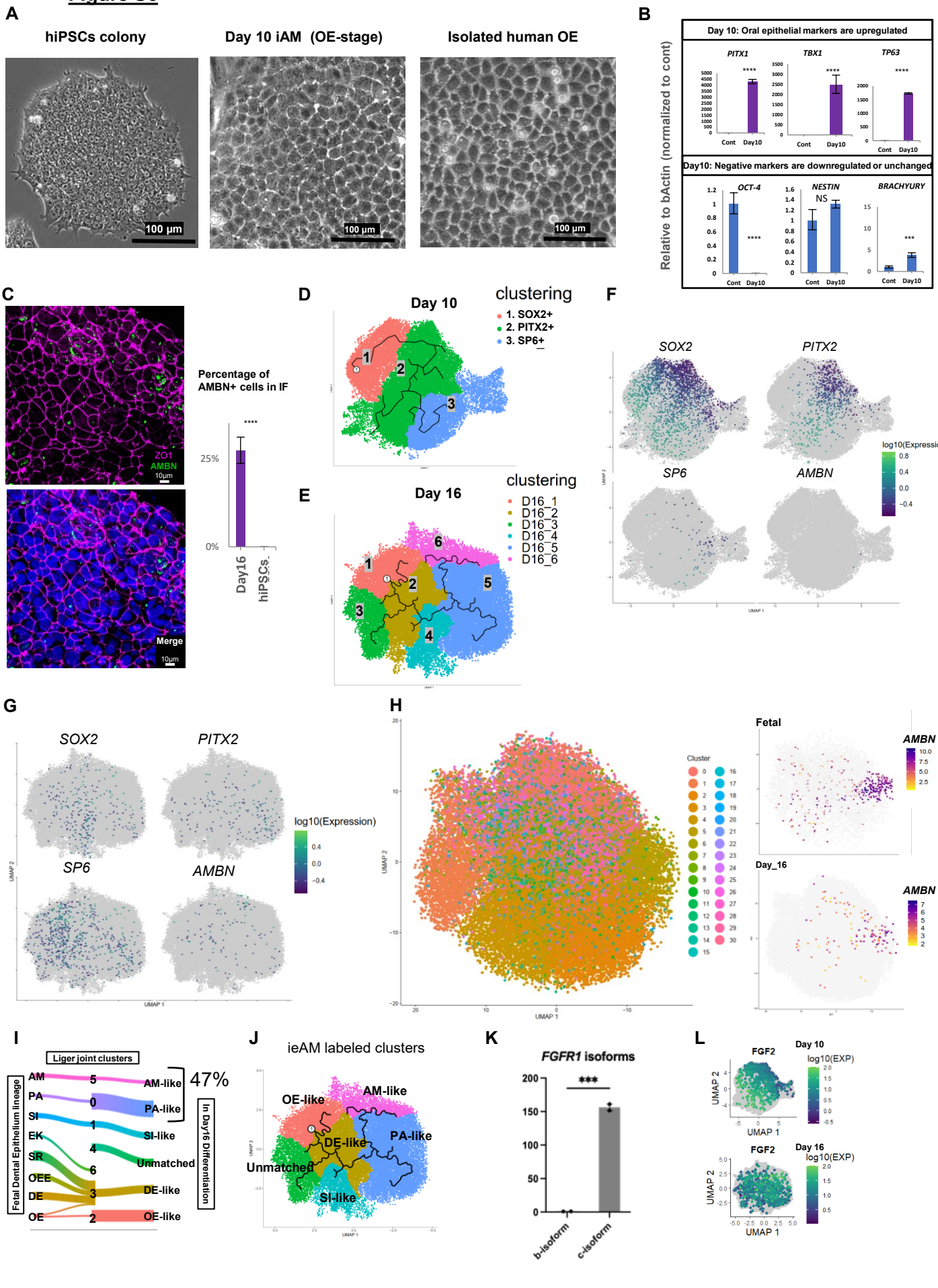
A
hiPSCs colony
Day 10 iAM (OE-stage)
Isolated human OE
100 µm
B
Day 10: Oral epithelial markers are upregulated
PITX1
TBX1
TP63
Relative to bActin (normalized to cont)
Cont
Day10
Day10: Negative markers are downregulated or unchanged
OCT-4
NESTIN
NS
BRACHYURY
C
ZO1
AMBN
Merge
10µm
Percentage of AMBN+ cells in IF
25%
0%
Day16
hiPSCs
D
Day 10
clustering
1. SOX2+
2. PITX2+
3. SP6+
E
Day 16
D16_1
D16_2
D16_3
D16_4
D16_5
D16_6
F
SOX2
PITX2
SP6
AMBN
log10(Expression)
G
UMAP 1
UMAP 2
H
Cluster
Fetal
Day_16
I
Liger joint clusters
Fetal Dental Epithelium lineage
AM
PA
SI
EK
SR
OEE
DE
OE
AM-like
PA-like
SI-like
Unmatched
DE-like
OE-like
47%
In Day16 Differentiation
J
ieAM labeled clusters
OE-like
AM-like
PA-like
DE-like
Unmatched
SI-like
K
FGFR1 isoforms
***
b-isoform
c-isoform
L
FGF2
Day 10
Day 16
log10(EXP)

Figure S7

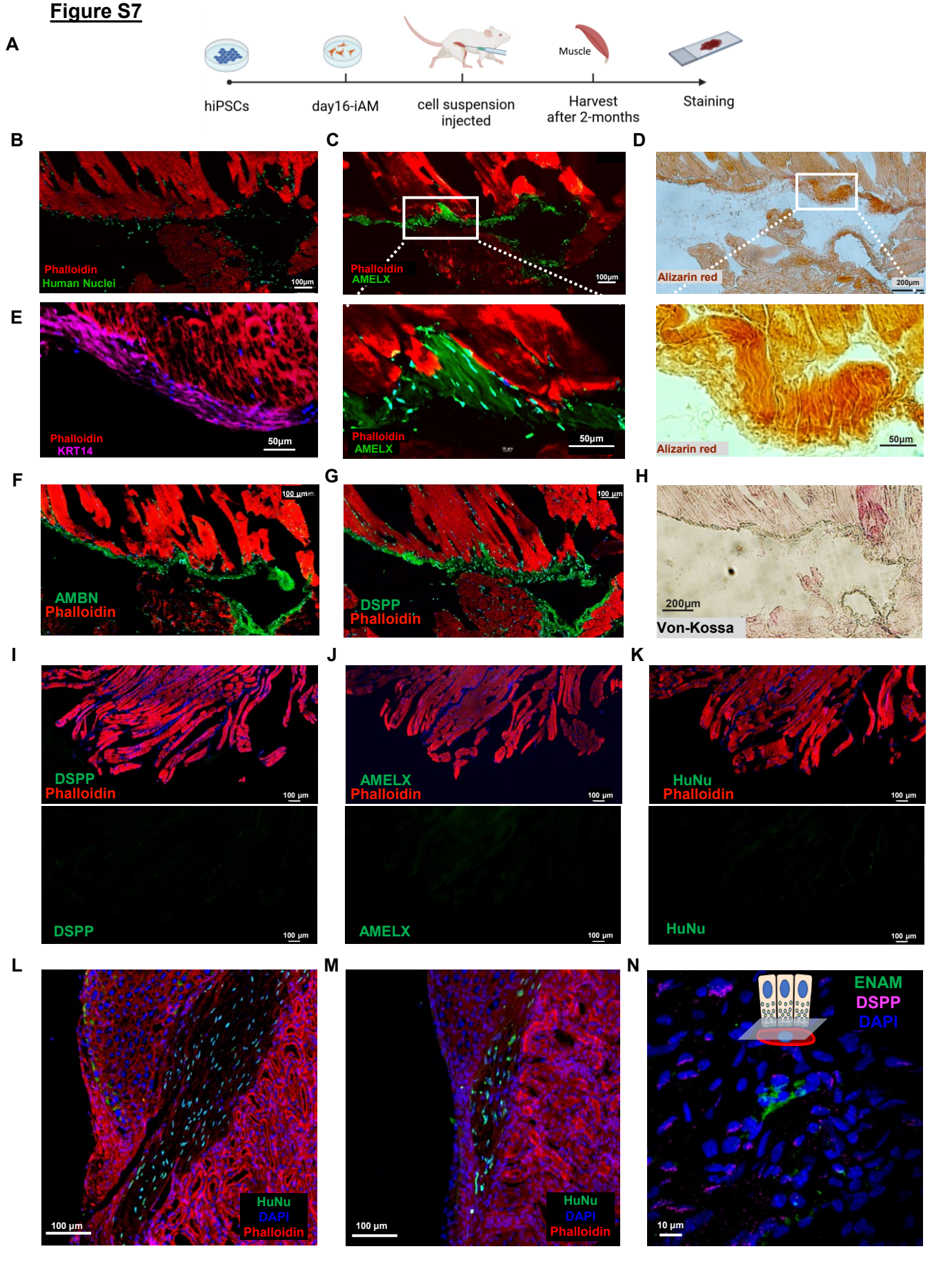
A
hiPSCs
day16-iAM
cell suspension injected
Muscle
Harvest after 2-months
Staining
B
Phalloidin
Human Nuclei
100μm
C
Phalloidin
AMELX
100μm
D
Alizarin red
200μm
E
Phalloidin
KRT14
50μm
Phalloidin
AMELX
50μm
Alizarin red
50μm
F
AMBN
Phalloidin
100 μm
G
DSPP
Phalloidin
100 μm
H
200μm
Von-Kossa
I
DSPP
Phalloidin
100 μm
DSPP
100 μm
J
AMELX
Phalloidin
100 μm
AMELX
100 μm
K
HuNu
Phalloidin
100 μm
HuNu
100 μm
L
HuNu
DAPI
Phalloidin
100 μm
M
HuNu
DAPI
Phalloidin
100 μm
N
ENAM
DSPP
DAPI
10 μm

Figure Legends:

Figure S1: A single-cell atlas of the developing human fetal jaws, teeth, and salivary glands tissues via sci-RNA-seq. (related to Figure 1)

(A) Depending on the tissue size at a given age, between 3 and 50 of each tissue sample were collected, pooled into 12 samples, and sent for sci-RNA-seq. (B) At 9-11gw, dissecting individual toothgerms or salivary glands in the bud stage was not feasible due to the large number of cells required to perform sci-RNA-seq protocol. Instead, jaws were separated into two segments of posterior jaw, containing jaw tissue distal of the canines (B, red boxes), and one segment of anterior jaw spanning from canine tooth to canine tooth region (B, blue box). At 12gw and beyond, individual toothgerms and submandibular salivary glands could be identified and isolated to be sequenced separately (C). Sequenced data was clustered, and the resulting plot revealed that each major tissue type occupied a specific region of the plot, with some shared support tissues localized in the center (D). Clusters were identifiable by the expression of known markers for each tissue type in heatmap (E). QC table for all sequenced data (F).

Figure S2: Expression of known marker genes for dental mesenchyme derived cell types (related to Figure 2)

Expression of known marker genes for each dental mesenchyme cell type shown in heatmap (A). Expression over time heatmap of dental follicle marker *IGFBP5* and subodontoblast markers *SALL1* (B). Gene plot of shared DP and DEM progenitor marker *PRRX1* (C). Cell cycle scoring of dental mesenchyme derived cell types (D). Mappings for dental mesenchyme-derived cell types at 13gw replicate (E) and 19gw replicate (F) identified by analysis of RNAScope images which show mapping for SOB, DF, DEM, OB, and POB cell types. Comparisons focused on the overlap between enriched marker genes of OB, SOB and POB with previously published datasets by Jing *et al* for postnatal mouse in (G), and by Krivanek *et al* for adult human dental pulp and apical papilla in (H). Gotrm analysis was done on the overlapped genes to highlight the common biological processes between OB in fetal human postnatal mouse in (I), and with adult human OB in (J).

Figure S3: Ameloblast developmental trajectory (related to Figure 3)

Expression of known markers at stages of dental epithelial lineage align with previously identified markers in each tissue and appear at expected developmental timepoints (A). Density of cells plotted by age demonstrating clusters enriched with more cells at a given timepoint (B). Gene plots and mean expression per cluster summary plots in UMAP space generated for the markers used to infer the logic table (File S3) which is used in the RNAScope mapping (C). The threshold expression per cluster was set to 25% of maximum expression per gene. Light green clusters considered as high expressing, dark blue as low expressing, and gray as low or no expression. Pathway analysis based on ligand receptor interaction highlighting the difference between SII and SIO (D) generated by *talklr*. Differential expressed between SII and SIO (E) used to generate GO terms to highlight the similarities and the differences between the two cell types. Mappings for dental epithelium-derived cell types in a stage matched (13gw of incisor) replicate sample (F) identified by analysis of RNAScope images showing the mappings for EK, OEE, IEE, CL, SII, and SRI cell types, and at (19gw of incisor) replicate sample (G) mappings for IEE, PA, SII, SIO, OEE, CL, SRI, SRO, eAM, and sAM cell types.

Figure S4: Spatial Expression of Odontoblast and Ameloblast Markers Differs Markedly from Early to Late Toothgerm Development (related to Figure 2 and 3)

Ameloblast markers amelogenin (AMELX) and ameloblastin (AMBN) expression begins in the early ameloblast after the early bell stage (A-H). Similarly, odontoblast marker dentin sialo phosphoprotein (DSPP) begins in the odontoblast after the early bell stage (I-K'), and early ameloblasts express low level of DSPP. However, Enamelin (ENAM) expression marks the secretory ameloblast (K-K'). Heatmaps of expression over time of AMELX (B), AMBN (F), DSPP (J) and ENAM (L). A table summarizing the protein expression level of the eAM, sAM and OB (M). Abbreviations: preodontoblast (POB), odontoblast (OB), preameloblast (PA), early ameloblast (eAM), secretory ameloblast (sAM), incisal edge (IE), cervical loop (CL). Scale bars: 100μm.

Figure S5: Pathway analysis in ameloblast trajectory (related to Figure 4)
(A) We developed a combined computations workflow to identify critical pathways at different developmental steps, represented by the schematic in (A), yielding a ranking and contribution to ameloblast differentiation for several major pathways (B) over several developmental stages. Using *talklr* ligand-receptor analysis, we identified the sources of the outgoing signals at early stages of ameloblast development (C-C'''). The top three pathways per stage are indicated in ligand:receptor interaction graphs (C). The thickness of the arrows indicates the number of unique possible interactions between clusters. The arrowheads indicate the receiver cells that express the receptors. Red arrows highlighting the interactions received by the cells of interest at each stage. Heatmaps are generated by first aggregating ligands gene expression for each cell, and then the average values are calculated per cluster (C″). Analyses demonstrate that at the placode stage, BMP and Activin signals come from the mesenchyme (DEM) to the epithelium while at the bud stage the oral and dental epithelium itself secrete WNT signals. In the early cap stages, WNT signals come from the dental epithelium while the mesenchyme secretes FGF and BMP signals toward the dental epithelium. At the late cap stage, following the development of the inner stellate reticulum (SRI), WNT signals switch to non-canonical WNT signaling from the SRI to the enamel knot (C‴).

Figure S6: Differentiation of human induced pluripotent stem cells (hiPSCs) into pre-ameloblasts (related to Figure 5)
(A) Brightfield images of hiPSCs, day 10 of *in vitro* differentiation, and isolated fetal oral epithelium after culturing for seven days (A) show that oral epithelium differentiated from iPSCs exhibit the same morphological characteristics as culture human oral epithelium. QRT-PCR (B) showed that compared to undifferentiated hiPSCs, differentiated oral epithelium exhibited elevated levels of known oral epithelium markers concomitant with a significant decrease in known pluripotency marker *OCT-4*. Additionally, the neuroepithelial marker *NESTIN*, and the early mesodermal marker *TBXT* (BRACHYURY) are relatively unchanged at day10 of the differentiation, indicative of a relatively lineage-specific differentiation. Successful further differentiation of oral epithelium into ameloblasts was demonstrated by immunofluorescence staining of day 16 (C), showing AMBN expression, and the membrane marker ZO1, with quantification analysis finding approximately 25% of cells positive for AMBN expression. Each study was performed in triplicate, with error bars representing ±SEM. Significance was determined by unpaired Student's t-test; ***$p < 0.001$; ****$p < 0.0001$. Day 10 (D) and Day 16 (E) samples were sequenced with sci-RNA-seq. Cells were clustered and analyzed to identify clusters with similar gene expression patterns to known cell types in fetal development (E). Gene expression density plots for known markers of different phases of ameloblast development show continuity between day 10 and day 16, with early markers *SOX2* and *PITX2* being predominantly expressed by day 10 (F) and shifting toward ameloblast-specific markers *AMBN* and *SP6* in day 16 (G). LIGER joint clustering analysis of Day 16 differentiation cells and the *in vivo* human fetal dental epithelium (Figure 3A) derived cells suggests the colocalization of *AMBN* expressing cells from in *vivo* and in *vitro* in cluster 6(H). LIGER joint clustering analysis suggests 47% of Day 16 cells share gene expression pattern of AM and PA (I), which allowed the labels to be transfer and annotate the cell type identity on iAM Day 16 differentiation UMAP graph (J). QRT-PCR (K) showed FGFR1 splice variant analysis in Day10 of ameloblast differentiation. FGF2 is abundantly expressed at day10/day16(L).

Figure S7: Characterization of iAM and formation of iAM/OB organoids (related to Figure 6)
(A) Schematic of the mouse *in vivo* experiments describing the steps for injecting day16-iAM subcutaneously into the left legs muscle of the adult SCID mice. The adult SCID mice at 2-month-old were dissected at the site of injection to perform further analysis to locate the cells such as immunofluorescence staining for human nuclear antigen in (B), AMELX (C), and Alizarin red staining showing mineralization (D), and KRT14 in (E), for AMBN (F) and DSPP (G). Von-Kossa staining for calcification was performed in a subsequent section in (H) showing black/brown staining localized to the injected cell region. Non-injection site muscles used as a negative control for the immunostaining DSPP (I), AMELX (J), HuNu (K). For the kidney capsule experiment, the injected cells were identified by HuNu staining (S7L–M), showing the survival of AM and OB-lineages. Immunofluorescence staining showing ENAM positive isAM, surrounded by DSPP positive DPSCs/OB in (N).